Interlayer correlation of embedded quantum-dot arrays through their surface strain energy distributions

Ernie Pan,[1,*] Yu Zou,[1] Peter W. Chung,[2] and Yan Zhang[1]
[1]*Computer Modeling and Simulation Group, College of Engineering, University of Akron, Akron, Ohio 44325, USA*
[2]*U.S. Army Research Laboratory, Aberdeen Proving Ground, Maryland 21005, USA*
(Received 6 June 2009; revised manuscript received 21 July 2009; published 17 August 2009)

We propose an interlayer correlation of multilayer quantum-dot (QD) distributions from a rigorous strain energy calculation. This leads to a map of correlations, or interlayer alignment, based solely on lateral and vertical spacing (*xdist*/*b* versus *hdist*/*h*). We identify four distinct correlation regimes—aligned correlation, antialigned correlation, noncorrelation, and the transition zone between the aligned and antialigned correlation. Our prediction matches well with available experimental data for a broad range of semiconductors with low elastic anisotropy $[A=2C_{44}/(C_{11}-C_{12})<2]$ and can further predict the QD array distribution for those with high elastic anisotropy ($A\geq 2$) by a simple shift in *hdist*/*h*. The agreement spans both IV-VI and III-V systems. Moreover, the aligned correlation regime produces a large decay in strain energy magnitudes in subsequently grown layers, which may contribute to their observed larger nucleation domains.

DOI: 10.1103/PhysRevB.80.073302 PACS number(s): 68.65.Ac

Distributions of strain energy density can induce a strong modification in the quantum-dot (QD) nucleation process on the depositing surface. Adatoms can accumulate at the strain minima on the surface,[1] and the minimum strain locations may reduce the barrier for three-dimensional island formation.[2] Both effects will result in the favored nucleation and growth of new QDs at the minima of strain energy density, which will lead to long-range spatial correlations in multilayer arrays.[3,4] To understand the influence of elastic fields on QD distributions, intensive experimental and numerical studies have been performed.[1,4–10] While the strain energy distribution for an isolated buried QD has been fully investigated, the single QD ignores the overlap of strain effects from the neighboring islands.[4–6] As for arrays of QDs, previous results are mainly based on experimental observations and are limited to the influence of the interlayer spacing.[1,7,8] The interaction energy of a sheet of buried two-dimensional islands based on the ratio of island width to lateral period was studied by Shchukin *et al.*[9] Employing the ratio between the vertical and lateral distances as the dominant parameter, Lévesque *et al.*[10] presented an interesting linear curve for the critical transition from aligned correlation to antialigned correlation where the influence of number of layers was not considered. While in most continuum simulation of QD array stacking only the point-QD model was used,[4,11,12] the kinetic Monte Carlo simulations were proposed to study the effect of the layer thickness on the QD size and its growth correlation.[13] Nevertheless, due to the complexity involved in the multiple tunable parameters associated with QD arrays, there have been no systematic investigations to date on their collective effects on the strain energy density and its correlation to the multilayer QD array distribution.

The objective of this Brief Report is a systematic calculation of the QD-induced strain energy density with respect to varying QD size and array stacking parameters (QD base *b*; QD height *h*; vertical spacer *hdist*; lateral (horizontal) spacer *xdist*; number of layers *n*) and the subsequent demonstration of their influence on the locations of newly formed QDs on the surface based on the resultant strain energy density distribution. By introducing the normalized lateral (horizontal) spacer versus vertical spacer (*xdist*/*b* versus *hdist*/*h*), we construct a correlation phase diagram containing four regimes separated by three (linear) curves that match well with existing experimental results. We present three key results: (i) for one embedded QD array, we vary the ratio *hdist*/*h*, *xdist*/*b*, *h*/*b* independently to investigate the dependence of strain energy density distribution; (ii) since the vertical alignment may dramatically affect the lateral ordering,[10,11] we then exploit the scaling behavior (*hdist*/*h* versus *xdist*/*b*) to predict the correlation regimes of the QD array, which motivates a phase diagram that agrees well with experimental results; (iii) finally, for fixed *hdist*, *xdist*, *h* and *b*, we vary the number of layers *n*, to investigate its effects on the correlation regimes. This could eventually provide a pathway to grow laterally ordered QD arrays.

The multilayer QD structure is modeled as a half-space substrate with embedded QDs. The surface strain energy density is obtained from the analytical Green's function method[14] combined with the Eshelby inclusion approach. The induced elastic strain γ_{kp}, stress σ_{ij}, and thus the strain energy density E at point $\boldsymbol{d}$ can be expressed as

$$\gamma_{kp}(\boldsymbol{d}) = \frac{1}{2}\gamma^*_{lm}C_{ijlm}\int_{\partial V}[U^{\boldsymbol{k}}_{j,d_p}(\boldsymbol{x};\boldsymbol{d}) + U^{p}_{j,d_k}(\boldsymbol{x};\boldsymbol{d})]\boldsymbol{n}_i(\boldsymbol{x})dS(\boldsymbol{x}), \tag{1}$$

$$\sigma_{ij}(\boldsymbol{d}) = C_{ijkp}[\gamma_{kp}(\boldsymbol{d}) - \chi\gamma^*_{kp}], \tag{2}$$

$$E(\boldsymbol{d}) = \frac{1}{2}\sigma_{ij}(\boldsymbol{d})\gamma_{ij}(\boldsymbol{d}), \tag{3}$$

where C_{ijkl} is the elastic stiffness tensor, $U^k_j(\boldsymbol{x};\boldsymbol{d})$ is the jth Green's elastic displacement at $\boldsymbol{x}=(x_1,x_2,x_3)$ due to a point force in the kth direction applied at $\boldsymbol{d}=(d_1,d_2,d_3)$; $n_i(\mathbf{x})$ is the outward normal on the boundary ∂V of the QD; γ^*_{ij} is the misfit strain; the subscript "," followed by the coordinates denotes the derivative; χ equals 1 if the observation point $\boldsymbol{d}$ is within the domain V and 0 otherwise. The integral on the

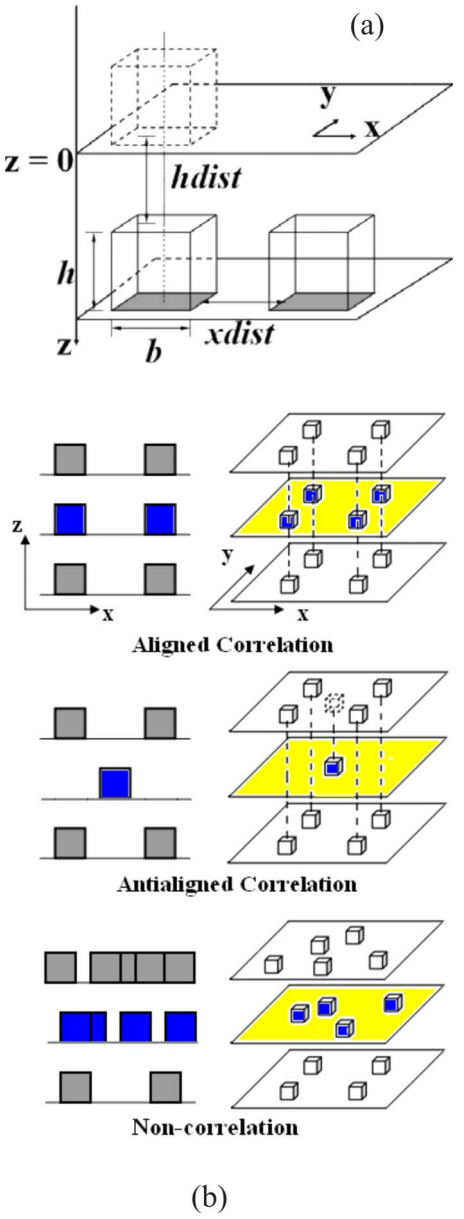

FIG. 1. (Color online) Schematic of multilayer QD array structure: (a) geometry of cubic QDs and (b) definition of three of the regimes (not including the transition zone)—aligned correlation, antialigned correlation, and noncorrelation.

surface of the QD can be carried out exactly on any flat element and the final expression for the strain energy density involves only a line integral over $\theta=[0,\pi]$.[14–16]

To extract the correlation regimes, it suffices to examine the half-space substrate with a buried QD array layer. For simplicity, we assume that the QDs are cubic in shape, as shown in Fig. 1(a). Based on the numerical calculations, we propose four correlation regimes for multilayer QD array and strain energy density—aligned correlation, a small transition zone, antialigned correlation, and noncorrelation, as schematically illustrated in Fig. 1(b). The term "antialigned" means that the minimum strain energy density on the surface is located between the projections of the buried QDs and "noncorrelation" means a random distribution of QDs. The sample material is InAs QDs within a GaAs (001) substrate.

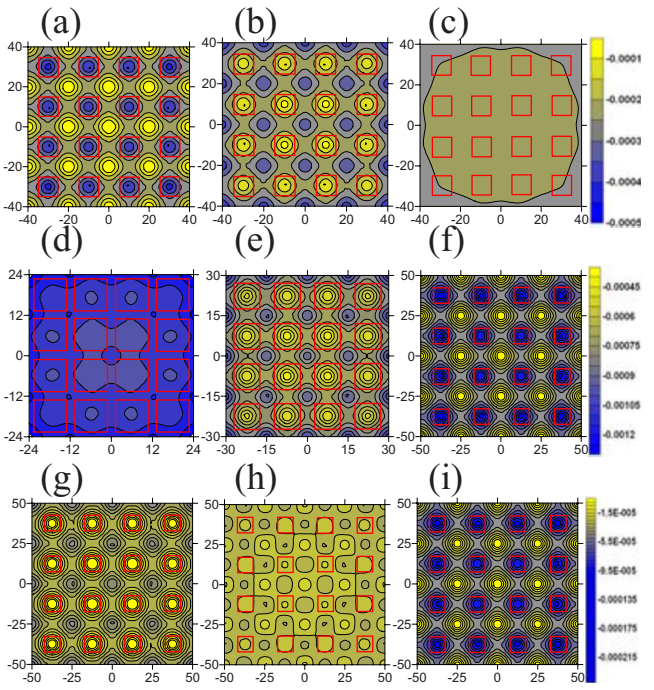

FIG. 2. (Color online) Strain energy density distribution (unit: 118.8×10^{15} N m^{-2}) on depositing surface. The horizontal and vertical axes (in nm) represent the two in-plane directions and the red squares represent the buried QD locations below the surface: (a)–(c) are for $hdist/h=0.8$, 1.5, and 2.5 (fixed $xdist=10$ nm and $h=b=10$ nm), corresponding to aligned correlation, antialigned correlation, and noncorrelation, respectively; (d)–(f) are for $xdist/b=0.2$, 0.5, and 1.5 (fixed $hdist=10$ nm and $h=b=10$ nm), corresponding to noncorrelation, antialigned correlation, and aligned correlation, respectively; (g)–(i) are for $b/h=5$, 1.25, and 1 (fixed $hdist+h=20$ nm, $xdist=15$ nm, and $b=10$ nm), corresponding to antialigned correlation, transition zone, and aligned correlation, respectively.

The misfit strain tensor in Eq. (1) is hydrostatic with $\gamma^*_{ij}=0.07\delta_{ij}$ and the elastic property of GaAs is taken from Pan.[15] The significance of the parameters [QD height h, base b to vertical (lateral) spacer $hdist$ ($xdist$)] on the correlation is addressed by the following three case studies:

Case (i): We first vary all dimensionless parameters for a QD array in a single layer. We assume a 10×10 cubic QD array and the resulting strain energy density distribution on the surface is plotted only in the 4×4 region due to periodicity. In the plots, the horizontal and vertical axes are the x and y directions (in nm). First, for fixed $xdist=10$ nm and $h=b=10$ nm, Figs. 2(a)–2(c) indicate that an increase in $hdist/h$ (0.8, 1.5, and 2.5) leads to a transition from aligned correlation to antialigned correlation which is consistent with experimental observation.[4,7,8,17] It is also observed that when $hdist/h$ exceeds a critical value, no correlation occurs (the noncorrelation regime) in the subsequent layer as indicated by the lack of any localized strain energy on the order of the QD spacing. Second, for fixed $hdist=10$ nm and $h=b=10$ nm, Figs. 2(d)–2(f) show that an increase in $xdist/b$ (0.2, 0.5, and 1.5) leads to a transition from antialigned correlation to aligned correlation which also agrees well with the experimental observation (Lévesque *et al.*[10]). In other

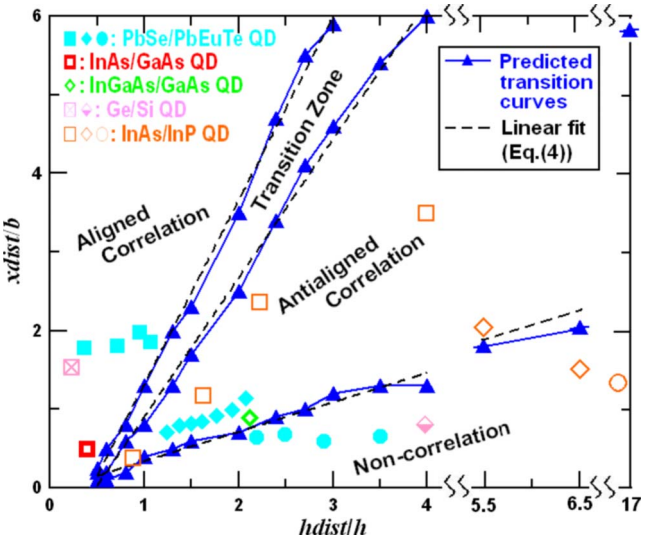

FIG. 3. (Color online) Four regimes (including the transition zone) of the surface QD locations based on the strain energy density distribution characterized by $xdist/b$ versus $hdist/h$. Solid lines denote the transition curves between the two adjacent regimes and the dashed straight lines are the best fits to these curves. Symbols refer to the experimental data where squares, diamonds, and circles denote the aligned correlation, antialigned correlation, and noncorrelation, respectively.

words, aligned correlation is favored for large lateral spacing while small $xdist/b$ facilitates antialigned correlation. Third, for fixed $hdist+h=20$ nm, $xdist=15$ nm, and $b=10$ nm, a decrease in aspect ratio b/h (5, 1.25, and 1) leads to a transition from antialigned correlation to aligned correlation as shown in Figs. 2(g)–2(i), which is also consistent with other independent numerical predictions.[12]

Case (ii): The scaling behavior of the correlated parameters is considered next. In addition to the vertical spacing, it is well known that the lateral distance between QDs plays a key role in pattern formation as demonstrated both theoretically[9] and experimentally.[18] Consequently, both vertical and lateral spacers are necessary to investigate the scaling behavior of strain energy density distribution. The correlation phases with respect to $hdist/h$ and $xdist/b$ are shown in Fig. 3 where there are the four regimes separated by three lines (solid lines from numerical calculation and dashed straight lines from curve fitting). It is interesting that our calculation indicates a transition zone (regime) between aligned correlation and antialigned correlation, which is consistent with previous studies.[1,17] The typical distribution of the strain energy density in this transition zone can be found in Fig. 2(h) where the locations of the minimum strain energy density are ordered but neither aligned nor antialigned. The transition state is in fact an offset shift of the minimum location along [100] and [010] directions, rather than [110] direction,[5,12] which means an oblique correlation with certain degree will be observed in experiments.

To verify the proposed QD correlation regimes, previous experimental results are added to Fig. 3. Available experimental results for PbSe/PbEuTe, InAs/InP, InAs/GaAs, InGaAs/GaAs, and Ge/Si QDs are from Springholz *et al.*,[17] Lévesque *et al.*,[10] Solomon *et al.*,[19] Gutiérrez *et al.*,[18] and

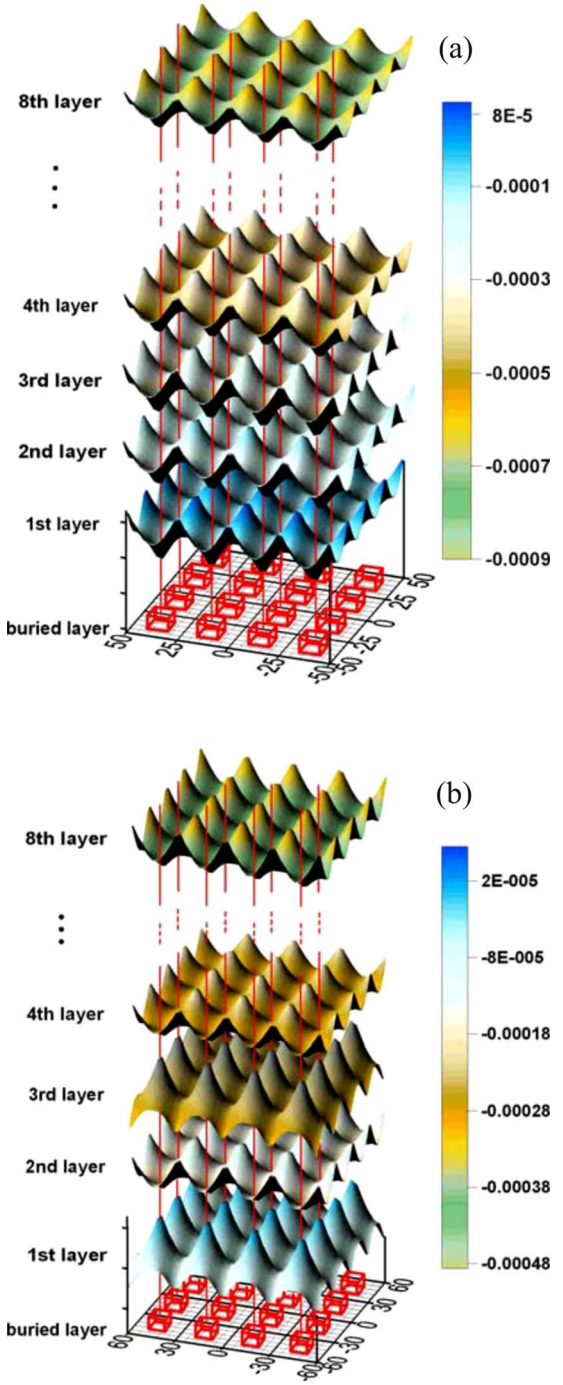

FIG. 4. (Color online) Strain energy density distribution (unit: 118.8×10^{15} N m^{-2}) on the depositing surface with one (first), two (second), three (third), four (fourth), and eight (eighth) layers of QD arrays. The red squares represent the original buried QD locations below the surface. Aligned correlation ($hdist=10$ nm; $xdist=15$ nm; $h=b=10$ nm) in (a) and antialigned correlation ($hdist=xdist=20$ nm; $h=b=10$ nm) in (b).

Kermarrec *et al.*[20] and are also plotted in Fig. 3 after conversion into the dimensionless parameters. It is noteworthy that the experimental data for semiconductors with low elastic anisotropy ratio ($A\approx0.27$, 1.56, and 1.83 for TeEuTe, Si, and GaAs) all fall into their expected regimes. For materials with high elastic anisotropy ($A\approx2.03$ for InP), one only needs to

TABLE I. Parameters in the three transition lines of Eq. (4).

		p_i	q_i
Line 1	Between aligned correlation regime and transition zone	2.33	−1.01
Line 2	Between transition zone and antialigned correlation regime	1.76	−0.85
Line 3	Between antialigned correlation and noncorrelation regime	0.37	−0.036

shift the horizontal $hdist/h$ value. In general, the three transition lines which separate the four regimes can be expressed by linear curve fits (for $i=1,2,3$),

$$xdist/b = p_i[hdist/h - (A+0.5)H(A-2)] + q_i, \qquad (4)$$

where p_i and q_i are the curve-fitting coefficients listed in Table I, A is the elastic anisotropy, and $H(x)$ is the Heaviside function for the right shift of the lines for materials with high anisotropy ($A \geq 2$).

Case (iii): The number of QD layers n is also an important parameter for the strain energy density distribution and the uniformity of the QD array.[6,18] To show the effect of the number of layers on the aligned and antialigned correlation regimes, the strain energy density distributions (unit: 118.8 $\times 10^{15}$ N m^{-2}) on the depositing surface with one (first), two (second), three (third), four (fourth), and eight (eighth) layers of QD arrays are shown in Fig. 4. The red squares represent the positions of the first buried QD layer beneath the surface. The aligned ($hdist=10$ nm; $xdist=15$ nm; $h=b=10$ nm) and antialigned correlations ($hdist=xdist=20$ nm; $h=b=10$ nm) are shown in Fig. 4(a) and Fig. 4(b), respectively. We notice further that, with increasing numbers of layers, the strain energy density magnitude decreases uniformly but the correlation qualitatively remains the same. Thus, for the antialigned correlation system, all even numbered layers are perfectly correlated among themselves and likewise for the odd numbered layers. Furthermore, the decrease in strain energy magnitude for each successive aligned correlated layer is faster than the decrease in successive antialigned correlated layers. Since a low strain energy density domain induces the nucleation of QDs (Refs. 1 and 2) the nucleation domain in aligned correlation regime will enlarge faster and easier than that in antialigned correlation regime. Thus, the faster decay in the strain energy magnitude [Fig. 4(a)] could be associated with the experimentally observed enlarged QD in aligned correlation.[1,7,18] Likewise, slower decay in antialigned correlation may explain the retarded QD expansion experimentally observed.[7,17]

In conclusion, we have systematically studied the strain energy density distribution on the depositing surface induced by buried QD arrays. A Green's function-based multilayer model predicts four regimes for nucleation arrangement—aligned correlation, antialigned correlation, noncorrelation, and aligned-antialigned transition. Our model also predicts the transition behavior between the regimes successfully solely in terms of the dimensionless variables $hdist/h$ versus $xdist/b$ for a broad range of QD systems including VI-IV and III-V materials. While our calculation agrees very well with previous experimental results for semiconductors with low elastic anisotropy, a shift can be introduced to predict the QD array correlation for materials with high elastic anisotropy. We further show that an increase in the number of QD layers decreases the strain energy magnitudes for both aligned and antialigned correlation regimes at different rates.

This work was partially supported by the National Natural Science Foundation of China Grant No. 10772106 (E.P.), and the Defense Threat Reduction Agency Joint Science and Technology Office (DTRA-JSTO) under Grant No. W911NF-06-2-0038 (P.W.C., E.P., Y. Zhang, and Y. Zou). We are also grateful to the Ohio Supercomputer Center for providing us with the required computer resource units under Grant No. PBS0268-2.

*pan2@uakron.edu

[1] Q. Xie, A. Madhukar, P. Chen, and N. P. Kobayashi, Phys. Rev. Lett. **75**, 2542 (1995).
[2] J. Tersoff, C. Teichert, and M. G. Lagally, Phys. Rev. Lett. **76**, 1675 (1996).
[3] A. A. Darhuber *et al.*, Appl. Phys. Lett. **70**, 955 (1997).
[4] G. Springholz, M. Pinczolits, V. Holy, S. Zerlauth, I. Vavra, and G. Bauer, Physica E **9**, 149 (2001).
[5] V. Holy, G. Springholz, M. Pinczolits, and G. Bauer, Phys. Rev. Lett. **83**, 356 (1999).
[6] J. Stangl, V. Holy, and G. Bauer, Rev. Mod. Phys. **76**, 725 (2004).
[7] X. D. Wang, N. Liu, C. K. Shih, and S. Govindaraju, Appl. Phys. Lett. **85**, 1356 (2004).
[8] X. B. Niu, Y. J. Lee, R. E. Caflisch, and C. Ratsch, Phys. Rev. Lett. **101**, 086103 (2008).
[9] V. A. Shchukin, D. Bimberg, V. G. Malyshkin, and N. N. Ledentsov, Phys. Rev. B **57**, 12262 (1998).
[10] A. Lévesque, N. Shtinkov, R. A. Masut, and P. Desjardins, Phys. Rev. Lett. **100**, 046101 (2008).
[11] G. Springholz, V. Holy, M. Pinczolits, and G. Bauer, Science **282**, 734 (1998).
[12] R. Kunert, Ph.D. dissertation, Technischen Universität, Berlin, 2006.
[13] M. Meixner and E. Scholl, Phys. Rev. B **67**, 121202(R) (2003); E. Pan, R. Zhu, and P. W. Chung, Proc. Inst. Mech. Eng., Part N, J. Nanoeng. Nanosyst. **218**, 71 (2005).
[14] C.-Y. Wang, M. Denda, and E. Pan, Int. J. Solids Struct. **43**, 7593 (2006); E. Pan, Y. Zhang, P. W. Chung, and M. Denda, Comput. Model. Eng. Sci. **24**, 157 (2008).
[15] E. Pan, J. Appl. Phys. **91**, 6379 (2002).
[16] E. Pan, Proc. R. Soc. London, Ser. A **458**, 181 (2002).
[17] G. Springholz *et al.*, Phys. Rev. Lett. **84**, 4669 (2000).
[18] M. Gutiérrez, M. Herrera, D. González, R. García, and M. Hopkinson, Appl. Phys. Lett. **88**, 193118 (2006).
[19] G. S. Solomon, J. A. Trezza, A. F. Marshall, Jr., and J. S. Harris, Phys. Rev. Lett. **76**, 952 (1996).
[20] O. Kermarrec, Y. Campidelli, and D. Bensahel, J. Appl. Phys. **96**, 6175 (2004).